Design Algorithm for Unbalance Compensation for Magnetic Rotor–Bearing System

Shuo-Chih WEI* and Shyh-Leh CHEN**
*Department of Mechanical Engineering, National Chung-Cheng University
No. 168, Sec. 1, University Road, Minxiong Township, Chiayi County 621301, Taiwan (R.O.C.)
E-mail: weishuochih@gmail.com
** Department of Mechanical Engineering, National Chung-Cheng University
No. 168, Sec. 1, University Road, Minxiong Township, Chiayi County 621301, Taiwan (R.O.C.)
E-mail: imeslc@ccu.edu.tw

Abstract

Unbalance-induced vibrations remain a critical challenge in high-speed rotor systems supported by active magnetic bearings (AMBs). This study presents an optimization-based procedure for systematically designing the parameters of an Unbalance Force Rejection Controller (UFRC). The UFRC is capable of suppressing synchronous currents caused by rotor mass unbalance and resonance, thereby improving energy efficiency and reducing vibration-induced noise. The proposed method requires only four inputs: the system's sensitivity function, minimum and maximum operating speeds, and the allowable peak sensitivity. The proposed method is optimization-based, ensuring that the designed parameters are optimal with respect to the objectives and constraints. Furthermore, the method is nonparametric, it does not require a full system model and system parameters, making it highly suitable for industrial applications. The optimized UFRC parameters were experimentally validated on the shaft of a magnetically levitated chiller system. Results show that, after activating the UFRC, the magnitude of the control current was reduced by 67% compared to the case without compensation and approached the same level as static levitation, showing the effectiveness of the optimized parameters.

Keywords : Magnetic bearing, Magnetic levitation , Unbalance compensation, Unbalance force rejection control, Unbalance suppression

1. Introduction

Active magnetic bearing (AMB) plays an important role in high-speed rotating machinery due to its contactless feature. Since AMB is contact-free and lubrication-free, it is especially suitable for magnetically levitated energy storage flywheels (Olabi et al., 2021) and turbomolecular pumps (Noh et al., 2005). In practice, due to assembly tolerance and manufacturing imperfection, rotating systems are affected by unbalance forces. For magnetic rotor-bearing systems, this will cause higher energy consumption, larger shaft displacement, and vibration noise. Since magnetic bearing systems are capable of actively adjusting the system behavior through control algorithms, unbalance compensation algorithms were developed to solve this problem. Unbalance compensation algorithms can be categorized into two categories based on the objective. The first category is unbalance vibration cancellation. The goal of this category is to control the magnetic bearing so that the rotor rotates about its geometric center, achieving higher position accuracy at the cost of higher energy consumption. The second category is unbalance force cancellation, also known as the unbalance force rejection control (UFRC). The goal of this category is to control the magnetic bearing so that the rotor rotates about its mass center, that is, principal axis. In that way, the energy consumption can be significantly reduced and vibration noise will be eased. In this study, we focus on the second category, that is, unbalance force cancellation.

For the second category, researchers utilized the generalized notch filter to achieve UFRC and proposed the stability criterion for the notch filter design in an insightful way (Herzog et al., 1996). The stability range for the parameter design can be determined based on the sensitivity function of the system. Also, the compensation effect for the notch filter at

different locations in the control loop were investigated (Zheng et al., 2016). A new structure that can not only achieve unbalance force rejection, but also suppress resonant vibrations was proposed (He et al., 2020). To deal with the stability issue introduced by the notch filter, researchers proposed a novel generalized notch filter for harmonic suppression control and aimed to improve the stability of the system (Gallego et al., 2021). The stability was improved and current consumption was significantly reduced. An unbalance vibration suppression method based on the sliding mode observer (SMO) and adaptive compensation has been proposed (Liu and Liu, 2016). Since the SMO is robust against the parameter uncertainties, the adaptive compensation based on the improved generalized notch filter can automatically compensate the uncertainty of the power amplifier dynamics. The effectiveness was verified on a magnetically suspended control moment gyro (MSCMG). However, none of these researches provides a clear guide on how algorithm parameters should be designed.

In this paper, we propose a systematic procedure for designing the parameters of a UFRC. The controller parameters are determined through an optimization-based procedure to ensure that the system meets the objectives. The proposed method aims to optimize the UFRC parameters such that two key objectives can be achieved: fast convergence and a sufficient stability margin. First, the influence of each parameter on the objectives is analyzed, and the corresponding design constraints are established. Based on this analysis, a fitness function is designed and optimization is performed to identify the parameter set that maximizes the fitness value. The main advantage of using an optimization approach is that the resulting parameters are guaranteed to be optimal with respect to the defined objectives and constraints. Furthermore, the method is nonparametric, which means that it does not require a detailed system model or parameter identification, making it particularly suitable for industrial applications where precise modeling is difficult. In addition, thanks to advances in computing technology, optimization procedures can now be executed with high computational efficiency. A systematic design method facilitates specific tailored parameters for each operation. When the controller parameters are adjusted, the corresponding UFRC parameters can be automatically updated using the proposed algorithm within a short time, while still satisfying stability requirements and ensuring fast convergence.

2. The magnetic rotor-bearing system under study

The system under study is a magnetic rotor-bearing system as shown in Fig. 1. The radial active magnetic bearings are denoted as ①, the position sensors are denoted as ②, the axial active magnetic bearing is denoted as ③ and the shaft is denoted as ④. The coordinate definition is depicted in Fig. 1 and the definition of each symbol is shown in Table 1. The dynamics of the rotor can be described using either sensor coordinate or center of mass (c.m) coordinate:

$$\begin{cases} \{x_f, x_r, y_f, y_r\}, & \text{for sensor coordinate} \\ \{\beta, x, -\alpha, y\}, & \text{for c.m coordinate} \end{cases} \tag{1}$$

The detailed derivation of the equation of motion is in the book by Maslen et al. (2009) and will be omitted here.

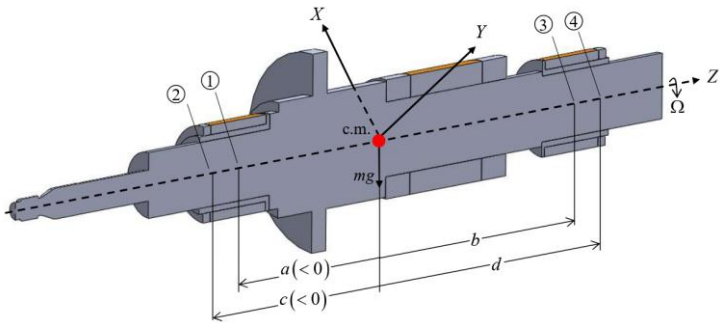

Fig. 1 Coordinate definition. c.m is the center of mass. ①: front bearing plane, ②:front sensor plane, ③:rear bearing plane, ④:rear sensor plane.

Table 1 Symbols and their definition.

Symbol	Definition
$-a$	Distance from c.m to front bearing plane
$-c$	Distance from c.m to front sensor plane
b	Distance from c.m to rear bearing plane
d	Distance from c.m to rear sensor plane
β	Rotational displacement with respective to Y axis
α	Rotational displacement with respective to X axis
x	Translational displacement with respective to X axis
y	Translational displacement with respective to Y axis
x_f	Displacement in X axis at front sensor plane
x_r	Displacement in X axis at rear sensor plane
y_f	Displacement in Y axis at front sensor plane
y_r	Displacement in Y axis at rear sensor plane

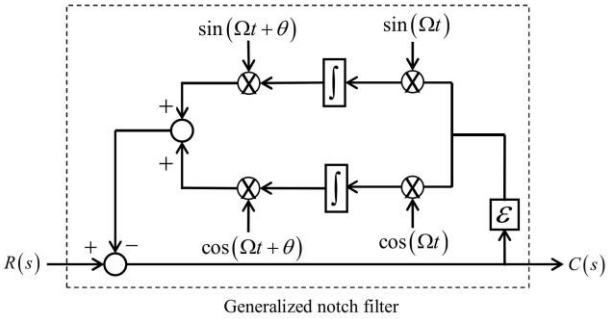

Fig. 2 Block diagram of generalized notch filter. ε and θ are parameters to be designed. Ω is the central frequency for the GNF and is the rotation speed of the rotor in this study.

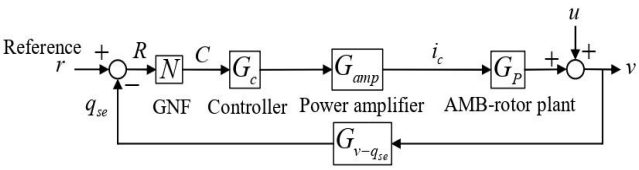

Fig. 3 One DOF block diagram. Each DOF is considered decoupled to simplify the problem. i_c is the control current, u is the unbalance vibration, v is the state used to describe the dynamics of the rotor and can be either in sensor coordinate or c.m coordinate, q_{se} is the rotor's response in sensor coordinate. $G_{v-q_{se}}$ is the coordinate transformation from v to q_{se}.

3. Review of unbalance force rejection control (UFRC)

Magnetic rotor-bearing systems, particularly those utilizing AMBs, are widely adopted in high-speed rotating machinery due to their non-contact feature, and long lifespan. However, unbalance forces can induce significant vibrations, compromise system stability, and increase power consumption. In addition, unbalance forces grow with the square of the rotation speed, the faster the rotation speed, the more severe the problem becomes. To solve this, UFRC emerged. The UFRC actively compensates for periodic forces caused by rotor unbalance, thereby improving energy efficiency and reducing vibration noises. A common way to achieve UFRC is by introducing a notch filter into the control loop (Herzog et al., 1996 and Zheng et al., 2016 and He et al., 2020). In this section, we will focus on what other studies have done on research about UFRC.

3.1 Generalized notch filter (GNF)

To implement UFRC, instead of using a conventional notch filter, this study adopted generalized notch filter (GNF) to gain more flexibility in shaping the frequency response. The GNF used in this study is identical to (Zheng et al., 2016). The block diagram of GNF is shown in Fig. 2 and its transfer function is

$$N(s)=\frac{C(s)}{R(s)}=\frac{s^2+\Omega^2}{s^2+\varepsilon\cos\theta s+\Omega^2-\Omega\varepsilon\sin\theta} \tag{2}$$

where Ω is the central frequency of GNF, θ and ε are parameters to be designed. The detailed derivation of the transfer function is in (Zheng et al., 2016) and will be omitted here.

3.2 Block diagram including GNF

In this research, the GNF is placed after the feedback signal and before the controller, as shown in Fig. 3. To understand the mechanism of UFRC, let us consider the case where the central frequency of the GNF is equal to the

rotation speed Ω_{rot} . Due to the fact that

$$N(s)\big|_{\substack{s=j\Omega_{rot}\\ \Omega=\Omega_{rot}}} = 0 \tag{3}$$

Any signal with frequency Ω_{rot} will be stopped by the GNF. In addition, since the unbalance force is synchronous to the rotation speed, the displacement induced by the unbalance force will be eliminated without entering the controller. Therefore, the current acquired by the controller can be significantly reduced and will not grow with the rotation speed.

3.3 Stability criterion of the closed-loop system

Adding a generalized notch filter to the loop seems like a simple way to achieve UFRC. However, since we have added a new block, the closed-loop system might not preserve its stability. Therefore, the generalized notch filter has to be designed carefully in order to stabilize the closed-loop system. Since the whole system involves several blocks, trying to define a stable parameter region in a parametric way, for example, knowing each block parameter and applying Routh-Hurwitz criterion, can be a nightmare. Thankfully, an insightful way of dealing with this problem was proposed (Herzog et al., 1996). The stability criterion for the GNF parameters can be determined simply using the frequency response of the sensitivity function of the original closed-loop system. The stability criterion is:

$$\begin{aligned} &-90^\circ < \theta + \arg(S_0(j\Omega)) < 90^\circ \\ &\quad (0 < \varepsilon \ll \min(\Omega)) \end{aligned} \tag{4}$$

where θ is the phase shift parameter for the GNF, Ω is the central frequency for the GNF and S_0 is the sensitivity function of the original closed loop system. Note that Eq. (4) is valid as long as $\varepsilon \ll \Omega$. This provides an important foundation for designing the GNF.

4. The design algorithm for UFRC parameters

As mentioned in the introduction, the goal of this study is to propose a systematic way, or algorithm, to design the parameters for unbalance compensation. To make the algorithm adaptive to all kinds of different systems and make it easy to implement, we take the optimization approach. That is, with given constraints and objective, we want to find the best GNF parameters using optimization algorithms, for example, particle swarm optimization (PSO), generic algorithm (GA), etc. This section is divided into 4 subsections. First, the objective and constraints of the optimization process are defined. Second, 1-DOF block diagrams are introduced to formulate the problem. After that, we quantify the influence of each parameter on the objective. Finally, a fitness function is designed based on the quantified result and the flow chart of the algorithm is established.

4.1 Objectives and constraints

The first objective is to achieve a fast convergence speed of the unbalance compensation. That is, once the unbalance compensation is activated, we want to achieve an instantaneous current reduction effect. In that way, the system can respond faster to any changes, including variation of rotation speed during acceleration and deceleration phases. The second objective is to achieve a good stability margin. The stability margin for a control system can be quantified using the maximum of its sensitivity function, called the peak sensitivity. Thorough regulation on the peak sensitivity level and how sensitivity should be measured for AMB-rotor systems are well established in ISO 14839-3. We have three constraints: constraint on θ , constraint on ε and constraint on peak sensitivity. The first two are based on the stability criterion, that is:

$$\begin{cases} \theta : -90^\circ < \theta < 90^\circ \\ \varepsilon : 0 < \varepsilon \ll \min(\Omega) \end{cases} \tag{5}$$

where S_0 is the sensitivity function of the original closed loop system. For the peak sensitivity value, one can define a permissible peak sensitivity value PS_{permi} and ensure that the optimized closed loop has a peak sensitivity lower than this value. A reasonable choice will be $PS_{permi} > \max(|S_0(j\omega)|)$. That is, the optimized peak sensitivity should be larger than the peak sensitivity of the original system. Thus, the third constraint is

$$PS < PS_{permi} \tag{6}$$

where PS is the peak sensitivity of the closed-loop system with GNF. From now on, when we refer to the system with GNF, we mean that the unbalance compensation is activated. When we refer to the original loop, we mean that the unbalance compensation is not activated.

4.2 The 1-DOF block diagram

To simplify the problem, we consider a 1 DOF block diagram. The output state can be the rotor response in either sensor coordinate or c.m coordinate; both cases share the same block diagram as shown in Fig. 3. The control current is denoted as i , u is the effect of unbalance and v is the state. If the output state is in the sensor coordinates, as in (Zheng et al., 2016), then

$$v \in \{x_f, x_r, y_f, y_r\} \tag{7}$$

Otherwise, $v \in \{\beta, x, -\alpha, y\}$. In addition, the only difference for these two representations is the structure of AMB-rotor plant:

$$G_P(s) = \begin{cases} \dfrac{k_i}{ms^2 + k_i}, & \text{for sensor coordinate} \\ \dfrac{1}{ms^2}, & \text{for c.m coordinate} \end{cases} \tag{8}$$

The rule of thumb for choosing the appropriate coordinate is that, with such a coordinate, the closed-loop dynamics can be treated as a decoupled system. Theoretically, systems with decoupled controller, also known as COG control, tend to use the c.m. coordinate to represent the system. On the other hand, systems with decentralized controller tend to use the sensor coordinate. Practically, by injecting an excitation signal into the loop in one DOF and observing how the rest of the DOFs respond, we can easily determine which coordinate should be used based on the coupling between them. For the system under study, we used the decoupled controller for levitation. During the experiment, it was found that no matter in the sensor coordinate or body coordinate, the coupling effect is insignificant. Therefore, for our system, both coordinates are possible options.

4.3 Quantify the objective

Before designing the fitness function, we need to understand how each parameter affects the objective first. The first objective is to achieve a fast response speed of the unbalance compensation. From Fig. 3, the transfer function from u to i is

$$T_{ui} = \frac{i(\mathrm{s})}{u(\mathrm{s})} = -\frac{NG_cG_{amp}}{1 + NG_L} \tag{9}$$

with loop transfer function $G_L = G_cG_{amp}G_P$. Since the real part of dominant poles of T_{ui} determines the convergence speed of i , the question now becomes how the GNF parameters affect the dominant poles of T_{ui} . Suppose $\varepsilon = 0$, we have

$$N(s) = \frac{s^2 + \Omega^2}{s^2 + \varepsilon\cos\theta s + \Omega^2 - \Omega\varepsilon\sin\theta} = 1 \tag{10}$$

Substituting Eq. (10) into Eq. (9), we know there will be poles at $\pm j\Omega$. From (Herzog et al., 1996), we know

$$\frac{\partial s}{\partial \varepsilon} = -\frac{1}{2}(\cos\theta + j\sin\theta)S_0(j\Omega) \tag{11}$$

This evaluates how the poles start from $\pm j\Omega$ vary if we increase ε . If ε is small, those poles near $\pm j\Omega$ are dominant poles. Since the convergence speed is determined by the real part of the dominant poles, we are interested in the real part of Eq.

(11). Rewrite Eq. (11) using Euler's formula,

$$\frac{\partial s}{\partial \varepsilon} = -\frac{1}{2} e^{j\theta} S_0(j\Omega) = -\frac{1}{2} M_s e^{j(\theta+\varphi_s)} \tag{12}$$

with $M_s = |S_0(j\Omega)|$, $\varphi_s = \arg(S_0(j\Omega))$. Therefore, the real parts are

$$\mathrm{Re}\{\left.\frac{\partial s}{\partial \varepsilon}\right|_{\substack{\varepsilon=0 \\ s=j\Omega}}\} = -\frac{1}{2} M_s \cos(\theta+\varphi_s) \tag{13}$$

Therefore, we know that increasing both ε and $M_s \cos(\theta+\varphi_s)$ results in faster convergence speed. In addition, with the stability criterion Eq. (5), we know that $0 \le \cos(\theta+\varphi_s) \le 1$ and $\varepsilon > 0$.

The second objective is to achieve a good stability margin. Since introducing GNF changes the characteristic of the system, we want to ensure that the resulting system still preserves a good stability margin. The peak sensitivity (PS) is defined as

$$PS = \max\left(\left|\frac{1}{1+G_L(j\omega)}\right|\right) \tag{14}$$

where $G_L(j\omega)$ is the loop transfer function. This is equivalent to finding

$$\min(|1+G_L(j\omega)|) \tag{15}$$

Eq. (15) calculates the closest distance from $G_L(j\omega)$ to -1, that is, the system being unstable. The larger the distance, the larger the stability margin and thus the smaller the PS, and vice versa. Therefore, we can quantify the stability of a system by calculating its PS. However, since the effects of the GNF parameters on PS are difficult to quantify, we took the numerical approach to ensure that the peak sensitivity is acceptable.

4.4 GNF design procedure

In order to meet all our objectives, the fitness function is designed first and the optimization is carried out to find GNF parameters that result in the highest fitness value. For UFRC, the parameter Ω for GNF is the rotation speed. In practice, the rotation speed varies. Therefore, the GNF is actually time varying. This means that for the same set of GNF parameters $\{\varepsilon, \theta\}$, the closed loop may be stable when the rotation speed is within some range but unstable in others. Therefore, it is crucial to determine the stable operating rotation speed for a given GNF parameter set $\{\varepsilon, \theta\}$.

The proposed design procedure is shown in Fig. 4. Only the block encircled by dashed box need to be determined whereas the rest can be carried out automatically. First, the algorithm will find an optimal $\{\varepsilon, \theta\}$ at $\Omega^* = \Omega_{\min}$. And then, the rotation speed Ω^* is increased gradually by $\Delta\Omega$ each step and check if this $\{\varepsilon, \theta\}$ meets all constraints. If any of the constraints are violated, the algorithm will go back and find the rotation speed at which the constraints are barely met. This rotation speed is the upper limit of the parameter set's operational speed range. The parameter set and this rotation speed is then denoted $\{\varepsilon_k, \theta_k, \Omega_k^*\}$, where the subscript k means that this is the k-th parameter set. After that, the algorithm will find an optimal $\{\varepsilon, \theta\}$ at $\Omega^* = \Omega_k$ and check if the constraints are met. This process undergoes iteratively until $\Omega^* \ge \Omega_{\max}$. The fitness function is designed as:

$$FT = \varepsilon_k M_s \cos(\theta_k + \varphi_s)\left(1 - \frac{PS}{PS_{permi}}\right) \tag{16}$$

with

$$\begin{aligned} &PS = \max\left\{\frac{1}{1+N_k G_0(j\omega)}\right\}, N_k = \frac{s^2 + \Omega^{*2}}{s^2 + \varepsilon_k \cos\theta_k s + \Omega^{*2} - \Omega^* \varepsilon_k \sin\theta_k} \\ &M_s = |S_0(j\Omega^*)|, \varphi_s = \arg(S_0(j\Omega^*)) \end{aligned} \tag{17}$$

Table 2 Optimized parameters for each DOF.

DOF	ε	θ(deg)
x_f	20.944	-60
x_r	20.944	-72.02
y_f	20.944	-64.43
y_r	20.944	-71.46

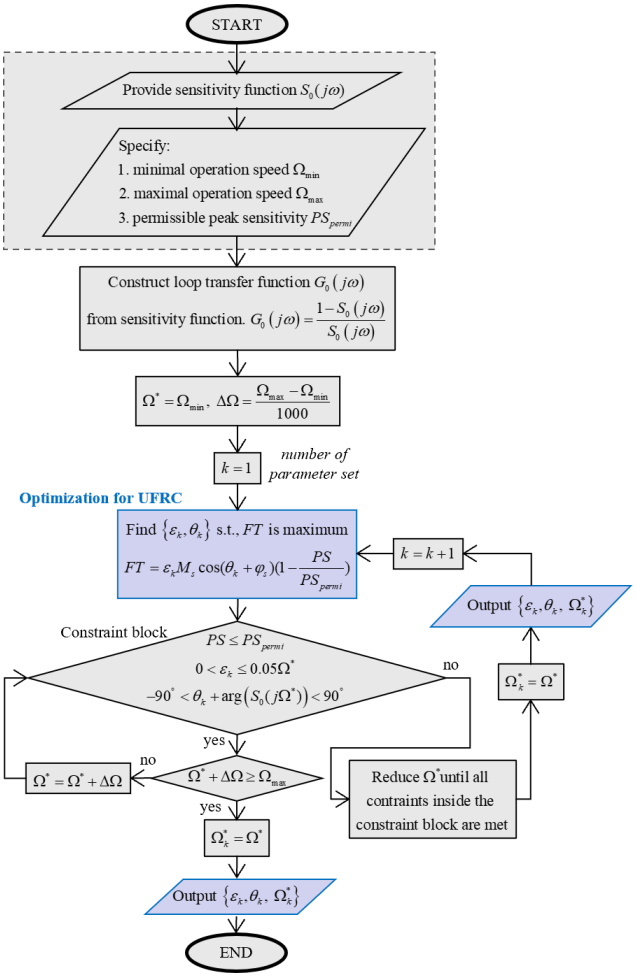

Fig. 4 The proposed design procedure. Starting from the top, the procedure takes four inputs that are encircled by a dash box. The loop transfer function is then calculated based on the sensitivity function and will be used in the optimization process later on. The optimization starts by setting rotation speed as Ω_{min} and find the optimal parameter set using the fitness function and the given constraints. Then the rotation speed is gradually increased by $\Delta\Omega$ to make sure that all the constraints are still met under this rotation speed. If any of the constraints are violated, the algorithm will go back and find the rotation speed at which the constraints are barely met and find another parameter set for this rotation speed. This process iterates until rotation speed reaches Ω_{max} .

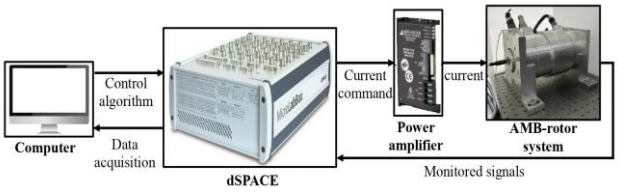

Fig. 5 The experimental setup.

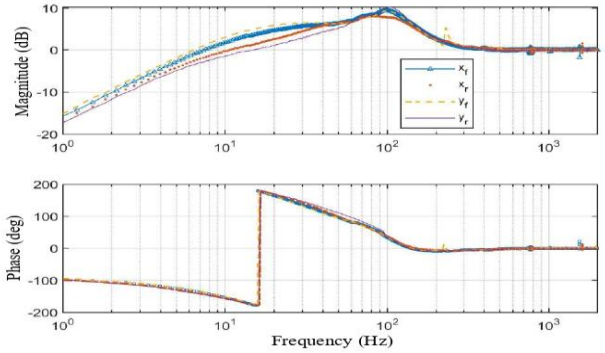

Fig. 6 Frequency response of the sensitivity function for the system under study.

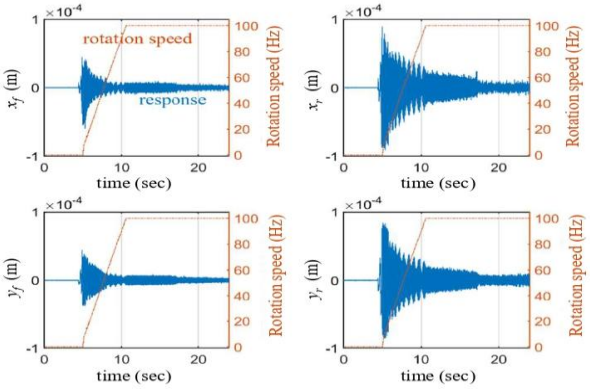

Fig. 7 Rotor displacement of each DOF v.s. rotation speed. The UFRC is turned on at 17 seconds. The displacement decreased slightly after activating the UFRC

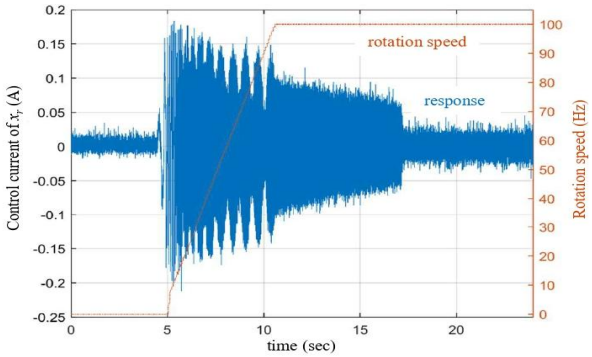

Fig. 8 Control current of x_r v.s. rotation speed. The UFRC is turned on at 17 seconds. The control current decreased significantly right after activating the UFRC.

5. Experimental result

The system used in the experiment rig is the shaft of a magnetically levitated chiller system as shown in Fig.5 and the experiment is conducted without any external load. The experimental setup is shown in Fig. 5. The control algorithm was deployed through MATLAB/Simulink and dSPACE. In order to control all five DOF motions, including four radial ones and one axial one, ten power amplifiers were used.

The 4 DOF sensitivity functions of the real system is shown in Fig. 6. The minimal and maximal operation speeds are set to 4000 RPM (66.67 Hz) and 20000 RPM (333 Hz), respectively. PS_{permi} for all 4 DOF are set to 10dB. The optimized GNF parameters for each DOF are shown in Table 2. Note that for each DOF, one set of parameter is enough to stabilize the system within the operation speed range. Figure 7 shows 4 DOF rotor displacements of the experiment result. Initially, the rotor is statically levitated, that is, levitated without rotating. Then, at around 8 seconds, the rotor starts to catch speed until the rotation speed reaches 100 Hz, as depicted in the figure. After the rotation speed is held at 100 Hz and the responses reached steady state, which is at 17 seconds, the UFRC is activated. A slight decrease in rotor vibration can be observed after UFRC was activated. Figure 8 shows the corresponding control current in one of the DOFs. As we can see, the current magnitude dropped by 67% after we activated the unbalance compensation and was about the same level as in the static levitation scenario. Thus, the effectiveness of unbalance compensation is verified.

6. Conclusion

In this study, we proposed a systematic procedure for designing the parameters of a UFRC. The proposed method requires only four inputs: the system's sensitivity function, minimum and maximum operating speeds, and the allowable peak sensitivity.

The proposed method is optimization-based, ensuring that the designed parameters are optimal with respect to the objectives and constraints. Furthermore, the method is nonparametric, which means that it does not require a detailed system model or parameter identification, making it particularly suitable for industrial applications where precise modeling is difficult. The design of the fitness function is based on two key objectives: fast convergence and a sufficient stability margin. The optimized UFRC parameters were experimentally validated on the shaft of a magnetic levitated chiller system. Results show that after the UFRC was activated, the vibration magnitude decreased and energy consumption significantly dropped. The magnitude of the control current was reduced by 67% compared to the case without compensation and approached the same level as static levitation, showing the effectiveness of the optimized parameters.

References

A. G. Olabi, T. Wilberforce, M. A. Abdelkareem, and M. Ramadan, "Critical review of flywheel energy storage system," Energies, vol. 14,no. 8, p. 2159, 2021.

M. D. Noh, S.-R. Cho, J.-H. Kyung, S.-K. Ro, and J.-K. Park, "Design and implementation of a fault-tolerant magnetic bearing system for turbomolecular vacuum pump," IEEE/ASME Transactions on Mechatronics, vol. 10, no. 6, pp. 626–631, 2005.

R. Herzog, P. Buhler, C. Gahler, and R. Larsonneur, "Unbalance compensation using generalized notch filters in the multivariable feedback of magnetic bearings," IEEE Transactions on control systems technology,vol. 4, no. 5, pp. 580–586, 1996.

S. Zheng, Q. Chen, and H. Ren, "Active balancing control of amb-rotorsystems using a phase-shift notch filter connected in parallel mode,"IEEE Transactions on Industrial Electronics, vol. 63, no. 6, pp. 3777–3785, 2016.

J. He, Z. Deng, C. Peng, and K. Li, "Reduction of the high-speedmagnetically suspended centrifugal compressor harmonic vibration usingcascaded phase-shifted notch filters," IEEE Sensors Journal, vol. 21,no. 2, pp. 1315–1323, 2020.

G. B. Gallego, L. Rossini, T. Achtnich, D. M. Araujo, and Y. Perriard, "Novel generalized notch filter for harmonic vibration suppression inmagnetic bearing systems," IEEE Transactions on Industry Applications,vol. 57, no. 6, pp. 6977–6987, 2021.

C. Liu and G. Liu, "Autobalancing control for mscmg based on sliding-mode observer and adaptive compensation," IEEE Transactions onIndustrial Electronics, vol. 63, no. 7, pp. 4346–4356, 2016.

E. H. Maslen, G. Schweitzer, H. Bleuler, and M. Cole, Magnetic bearings: theory, design, and application to rotating machinery. Springer,2009.